Experimental Validation of Wind Estimation Using a Micro-helicopter

Alexander B. Leishman* and Derek A. Paley†
University of Maryland, College Park, MD, 20742, USA

Autonomous air and ocean vehicles operating in real-world environments will frequently encounter flowfields such as wind and ocean currents. The ability of a vehicle to estimate the spatial variation of surrounding flows is useful for the collection of the flow data itself and for the feedback of the data into individual or cooperative control algorithms. This paper presents a novel flowfield estimator and, along with a previously developed estimator, tests the capability of wind estimation under non-ideal conditions. The testing was done through numerical simulation and physical experimentation using tracking data of a micro-helicopter flying through a fan-produced wind-field. Both estimators are based upon the model of a self-propelled Newtonian particle in a steady, uniform wind. Each estimator requires particle heading and position data for all time in order to produce a wind estimate. For error convergence, the estimators also require that the particle travel at a constant speed relative to the wind. Behavior of the estimators without the condition of wind uniformity is discussed. The estimators were tested experimentally, using a micro-helicopter and a fan-produced wind-field. Measurements of the position and orientation values of the helicopter along its flight path were taken with an infrared motion capture system. This data was run through the estimators and the resulting wind estimates are presented and compared to the measured wind-field. The trade-offs associated with each estimator are discussed and discrepancies between the theoretical model and the real-world conditions are addressed. Future estimator improvements and research directions are presented.

Nomenclature

$f_k(t)$	Flow/wind velocity at position r_k and time t
$\hat{f}_k(t)$	Estimated flow/wind velocity at position r_k and time t
i	Imaginary unit
K	Control gain
r_k	Position of particle k
$\hat{r}_k$	Estimated position of particle k
$\dot{r}_k$	Inertial velocity of particle k
$s_k(t)$	Speed of particle k at time t relative to the wind
u_k	Angular rate of change of the velocity orientation relative to the wind of particle k
$\hat{v}_k$	Estimated inertial velocity of particle k
θ_k	Orientation of the velocity of particle k relative to the wind

I. Introduction

Autonomous air and ocean vehicles operating in real-world environments will frequently encounter spatially varying flowfields (e.g. wind and ocean currents). A vehicle with the ability to estimate the spatial variation of surrounding flows is useful for the collection of the flow data itself and for the feedback of the

*Undergraduate Student, University of Maryland, College Park; leishman3@gmail.com. AIAA Student member.
†Assistant Professor, Department of Aerospace Engineering; dpaley@umd.edu. AIAA Associate Fellow.

data into individual or cooperative control algorithms. A team of vehicles with the ability to estimate the surrounding flow magnitude and direction would be capable of mapping three-dimensional flowfields by flying paths throughout a given measurement volume.

In this paper, we present a novel wind estimator that is capable of estimating both wind speed and the vehicle speed relative to the wind. This estimator, along with a previously derived wind estimator is tested using numerical simulation and real-world tests using a micro-Unmanned Aerial Vehicle (UAV). Peterson *et al.* developed a wind estimator requiring the condition of a constant vehicle speed relative to the wind.[1] We have developed an estimator that loosens this restriction, recognizing that it is not always feasible to ensure that the vehicle has a constant wind-relative speed when flying through a non-uniform wind-field.

Both estimators are based on a two-dimensional model of a self-propelled Newtonian particle traveling through a steady, uniform wind. The particle is defined as traveling at a constant speed relative to the wind and having a steering force perpendicular to its direction of travel. If the position and orientation of the particle is known for all time, both estimators can theoretically determine the magnitude of a steady, uniform wind.

We have validated both estimators through numerical simulation of a particle traveling through a uniform wind. Then, we simulated the estimators' behavior when the condition of spatial wind uniformity is not met– a more realistic scenario for a UAV.

We experimentally tested both estimators with a micro-UAV and analyzed the results to identify the validity of the particle model and estimators when operating in non-idealized, real-world conditions. An R/C micro-helicopter served as the test platform and was piloted through a wind-field produced by an array of box fans. The position and orientation of the vehicle was tracked using an infrared, three-dimensional positioning system. The micro-helicopter took the role of the Newtonian particle in the aforementioned model and the tracking data was run through each estimator in order to obtain an estimate of the wind-field along the path of the helicopter. The resulting estimates are presented and compared to the measured values of the wind-field.

Section II presents a mathematical framework for the estimators. Section III presents the results from numerical simulation of the estimators and discusses the strengths and weaknesses of each. Section IV presents the experimental results and proposes research directions to improve the real-world implementability of the estimators and particle model.

II. Mathematical Framework for Wind Estimation

The micro-helicopter is modeled as a planar, self-propelled Newtonian particle k traveling through a wind-field at a speed s_k relative to the wind. The particle heading angle $\theta_k(t)$ and postion $r_k(t) \in \mathbb{C}$ are known for all time. Additionally, the value of θ_k can be controlled by a steering control perpendicular to the velocity of the particle. The velocity of the particle relative to the wind is assumed to be $s_k e^{i\theta_k}$, or rather, the velocity of the particle relative to the wind is always aligned with the heading of the particle (no side-slip). The wind velocity at the location of the particle at time t is defined as $f_k(t) = f_k(t, r_k)$ and is unknown. The inertial velocity $\dot{r}$ of particle k in the complex plane is therefore

$$\begin{aligned} \dot{r}_k &= s_k e^{i\theta_k} + f_k(t) \\ \dot{\theta}_k &= u_k \end{aligned} \tag{1}$$

A. Estimation of Position and Wind Velocity (Estimator 1)

Consider the case where s_k is known and unvarying and the wind $f_k(t) = f$ is steady and uniform. An estimate of the wind-field $\hat{f}(t)$ can be made using a dynamic estimate of the position $\hat{r}_k(t)$.[1]

The error values for the particle are defined as $e_1 = \hat{r}_k - r_k$ and $e_2 = \hat{f}_k - f_k$. The error dynamics are chosen to be

$$\begin{aligned} \dot{\hat{r}}_k &= s_k e^{i\theta_k} + \hat{f}_k(t) - K_1(\hat{r}_k - r_k) \\ \dot{\hat{f}}_k &= -K_2(\hat{r}_k - r_k) \end{aligned} \tag{2}$$

Where K_1 and K_2 are gains of the system. The error dynamics can be written as

$$\begin{aligned}\dot{e}_{1,k} &= s_k e^{i\theta_k} + \hat{f}_k(t) - K_1(\hat{r}_k - r_k) - s_k e^{i\theta_k} - f_k = -K_1 e_{1,k} + e_{2,k} \\ \dot{e}_{2,k} &= -K_2(\hat{r}_k - r_k) = -K_2 e_{1,k}\end{aligned} \tag{3}$$

In matrix form,

$$\begin{bmatrix}\dot{e}_{1,k} \\ \dot{e}_{2,k}\end{bmatrix} = \underbrace{\begin{bmatrix}-K_1 & 1 \\ -K_2 & 0\end{bmatrix}}_{\triangleq A}\begin{bmatrix}e_{1,k} \\ e_{2,k}\end{bmatrix} \tag{4}$$

If $K_1 > 0$ and $K_2 > 0$, then $Re\{\lambda(A)\} < 0$ and the system is exponentially stable. Choosing a gains $K_1 = 2\sqrt{K_2} > 0$ results in critical damping.

Proof. The eigenvalues of A are $\lambda = \frac{K_1 \pm \sqrt{4K_2 - K_1^2}}{2}$. Choosing $K_1 = 2\sqrt{K_2}$ results in $\lambda = -K_1$ with multiplicity two. The system is therefore critically damped due to the repeated negative, real eigenvalues.

B. Estimation of Position and Platform Velocity (Estimator 2)

Now, consider the case where the particle wind-relative speed s_k and wind magnitude $\|f_k\|$ are unknown. The position r_k and orientation θ_k are still known for all time. The model then becomes

$$\begin{aligned}\dot{\hat{r}}_k &= \hat{s}_k e^{i\theta_k} + \hat{f}_k \\ \dot{\theta}_k &= u_k\end{aligned} \tag{5}$$

where $\hat{s}_k$ and $\hat{f}_k$ are (dynamic) estimates.

For futher restriction, we examine the case where the vehicle speed s_k is constant and the wind $f_k = \beta \in \mathbb{R}$ is constant, uniform, and in a known direction with only its magnitude unknown. Let $\hat{v}_k = \dot{\hat{r}}_k = \hat{s}_k e^{i\theta_k} + \hat{\beta}$. Therefore

$$Re\{\hat{v}_k\} + iIm\{\hat{v}_k\} = \hat{s}_k \cos(\theta_k) + i\sin(\theta_k) + \hat{\beta} \tag{6}$$

equating the real and imaginary parts of (6) gives

$$\begin{aligned}\hat{s}_k &= \tfrac{Im\{\hat{v}_k\}}{\sin(\theta_k)} \\ \hat{\beta} &= Re\{\hat{v}_k\} - \hat{s}_k\cos(\theta_k) = Re\{\hat{v}_k\} - \cot(\theta_k)Im\{\hat{v}_k\}.\end{aligned} \tag{7}$$

Estimating s_k and β can now be achieved by estimating v_k. To do this, let $e_1 = \hat{r}_k - r_k$ (as in II.A) and $e_2 = \hat{v}_k - v_k$. This gives

$$\begin{aligned}\dot{e}_{1,k} &= \dot{\hat{r}}_k - \dot{r}_k = \dot{\hat{r}}_k - v_k \\ \dot{e}_{2,k} &= \dot{\hat{v}}_k - \dot{v}_k = \dot{\hat{v}}_k - s_k i e^{i\theta_k} u_k.\end{aligned} \tag{8}$$

Choosing

$$\begin{aligned}\dot{\hat{r}}_k &= \hat{v}_k - K_1(\hat{r}_k - r_k) \\ \dot{v}_k &= -K_2(\hat{r}_k - r_k),\end{aligned} \tag{9}$$

gives error dynamics

$$\begin{bmatrix}\dot{e}_{1,k} \\ \dot{e}_{2,k}\end{bmatrix} = \underbrace{\begin{bmatrix}-K_1 & 1 \\ -K_2 & 0\end{bmatrix}}_{\triangleq A}\begin{bmatrix}e_{1,k} \\ e_{2,k}\end{bmatrix} + \begin{bmatrix}0 \\ s_k i e^{i\theta_k} u_k\end{bmatrix}. \tag{10}$$

If $K_1 > 0$ and $K_2 > 0$, then $Re\{\lambda(A)\} < 0$, with the same critical damping as (4). In addition, if $u_k = 0$, then $e_1 = e_2 = 0$ is exponentially stable. Otherwise, if $u_k \neq 0$, then $e_1^2 + e_2^2$ is upper bounded by a linear function of the maximum of $|s_k u_k|$ over time. Regardless, the estimator will give a value $\hat{v}_k$ that can be used in (7) to calculated $\hat{s}_k$ and $\hat{\beta}$.

III. Numerical Simulation

A. Introduction

In this section, we use use computer simulation to verify both estimators and determine their effectiveness when the condition of flow uniformity is lifted. In Section III.B a time-invariant, uniform wind is used to verify the theoretical behavior of the estimators using the assumptions stated in Section II. In Section III.C we test the behavior of the estimators in a parabolic wind-field that is similar in profile to the actual wind-field produced by the fans in the experiment.

A simulator was created in MATLAB to model the behavior of the previously described self-propelled particle in a wind. The wind $f_k(t)$ and the values of $\theta_k(t)$ and s_k were given to the simulator and the differential equation for $\dot{r}_k(t)$ were integrated numerically using the ode45 function in MATLAB. The simulation was run so that the particle traveled a single path across the wind-field. In order to further match the model to the planned experiment, the heading angle θ_k was kept constant in the simulation because a yaw controller would be keeping the heading angle constant during experimentation (Section IV.A). Additionally, s_k was kept constant, per the assumption of the derivations in Section II.

B. Estimation of a Time-invariant, Uniform Wind

The position data from the simulation, along with the values of s_k and θ_k were processed with Estimator 1 using the critically damped gains $K_1 = 10$ and $K_2 = 25$ (Section II.A). The estimator behaved as expected, with e_1 and e_2 quickly converging to zero.

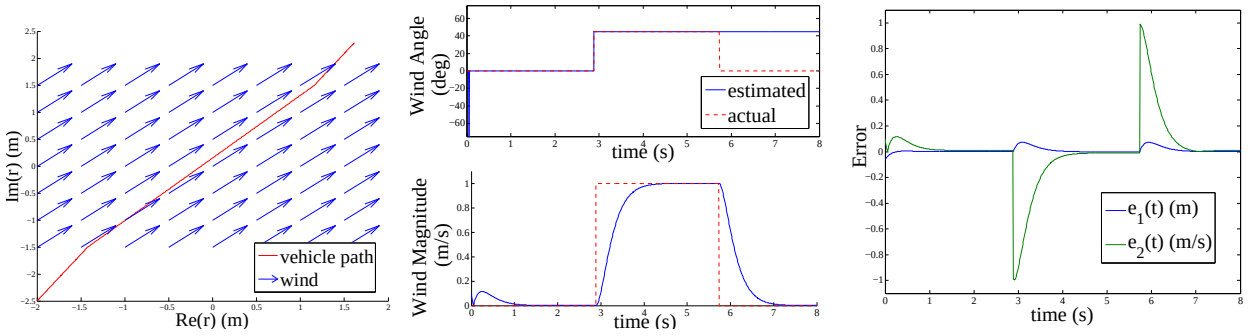

(a) Simulated wind and particle path (b) Estimated angle and magnitude (c) Error behavior

Figure 1. Simulation results for Estimator 1 in a uniform wind

Figure 1 shows the path and wind estimation results for a particle traveling in a plane with a 3 meter wide uniform wind-field of unit magnitude at an angle of 45° from the real-axis ($f = e^{\frac{\pi}{4}i} m/s$). The particle is traveling at a speed $s_k = 0.4$ m/s relative to the wind with a constant heading $\theta_k = 60°$. The particle began and ended its path outside of the wind, which caused the wind to act as a step input to the estimator when the particle crossed the flow boundary. Additionally, the initial values of r_k and f sent to the estimator were offset from the actual values in order to further verify the convergent behavior of the estimator. The particle started at a position of $r_k = -2 - 2.5i$ m with an initial velocity $v_k = 0.5 + \frac{\sqrt{3}}{2}i$ m/s. However, the initial position and wind values sent to the estimator were $r_{k,0} = -1.9 + 2.5i$ m and $f_0 = 0.1 + 0i$ m/s.This initial error can be seen in the peak of the magnitude estimate during the first few seconds of data (Figure 1(b)). The angle estimation outside of the wind is purely a result of the numerical behavior of ode45 because when there exists no wind, there exists no wind angle.

Estimator 2 was then tested under uniform wind conditions. Due to the directional restriction of the estimator, the direction of wind must be along the real axis (Section II.B). The gains were again set to the critically damped values of $K_1 = 10$ and $K_2 = 25$. It is important to note that although the estimator is different, the steady state error dynamics (Equation 10) remain the same. The particle started at a position of $r_k = -2 - 2.5i$ m with an initial velocity $v_k = 0.5 + \frac{\sqrt{3}}{2}i$ m/s. However, the initial values sent to the estimator for r_k and v_k were again offset from the actual values: $r_{k,0} = -1.9 + 2.5i$ m and $v_{k,0} = 0.1 + 0i$ m/s respectively.

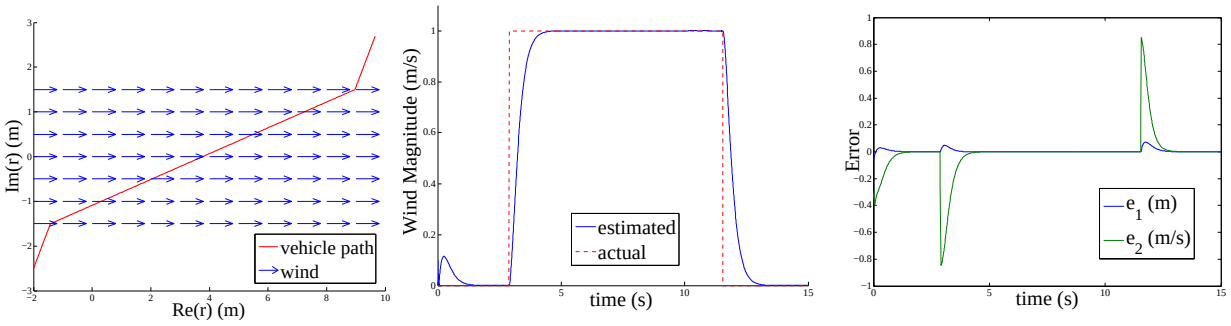

(a) Simulated wind and particle path (b) Estimated wind magnitude (c) Error behavior

Figure 2. Simulation results for Estimator 2 in a uniform wind

As seen in Figures 2(b) and 2(c), the estimator behaved as expected, quickly reaching a steady state of zero for both errors. Again, the abrupt change in wind magnitude at the field boundary acted as a step input into the estimator and the solution quickly converged. It is important to note that the error values e_1 and e_2 have the same units for both estimators, but the parameter being estimated for e_2 is different (Section II).

C. Estimation of Steady, Non-uniform Wind

Now, we consider the case where the wind is no longer uniform. A parabolic shaped wind-field (Figure 3) was used in the simulation because this is the shape of the magnitude profile of the actual wind from the fans used in the experiment. The particle parameters were kept the same. The behavior of the estimator using the critically damped gains can be seen in Figure 4.

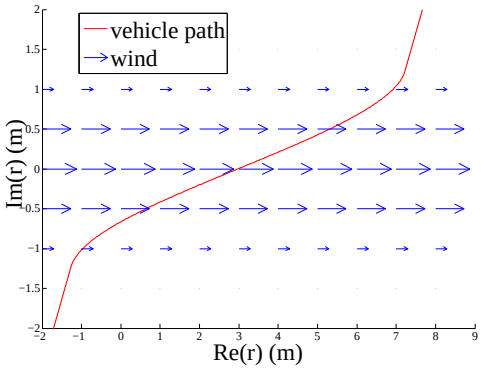

Figure 3. Simulated wind and particle path

The values of the magnitude of $\hat{f}_k$ lag the actual values in time. This lag can be greatly reduced by increasing the value of K_2 relative to K_1. However, this introduces overshoot in the estimator (Figure 5). In this case, the gains were set to $K_1 = 3.5$ and $K_2 = 35$. This improvement in the estimation accuracy can be explained through Lyapunov analysis of the estimator dynamics, which shows that in general, $K_2 >> K_1$ will lead to a faster estimator response.[2]

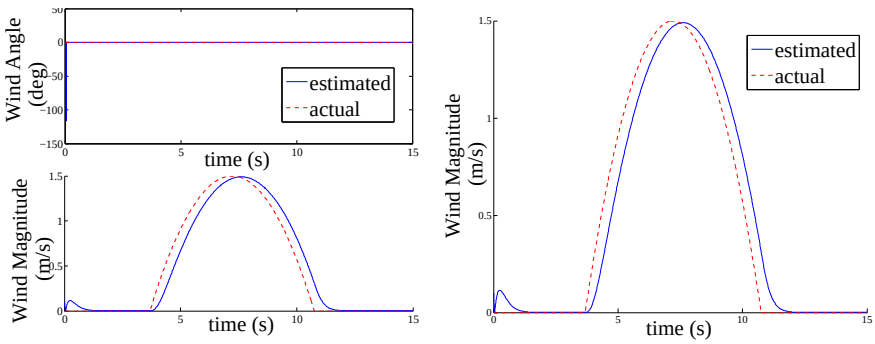

(a) Estimator 1 results

(b) Estimator 2 results

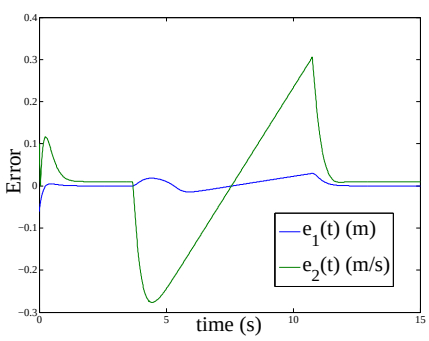

(c) Estimator 1 error

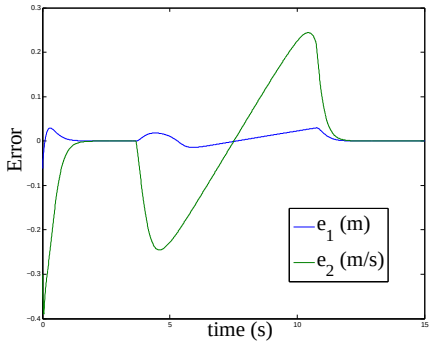

(d) Estimator 2 error

Figure 4. Estimated wind and error results for non-uniform wind-field ($K_1 = 10, K_2 = 25$)

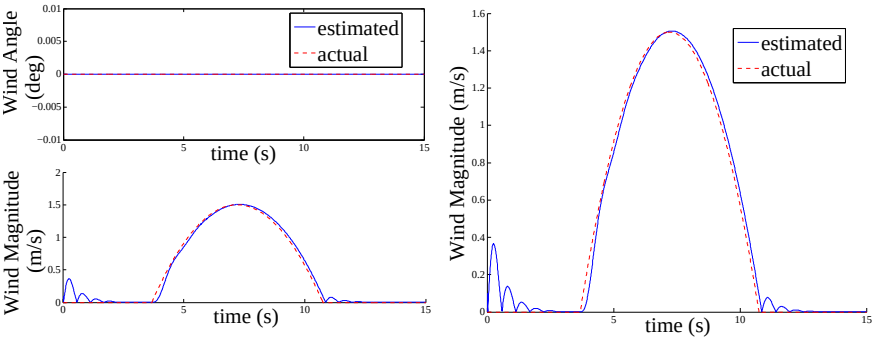

(a) Estimator 1 results

(b) Estimator 2 results

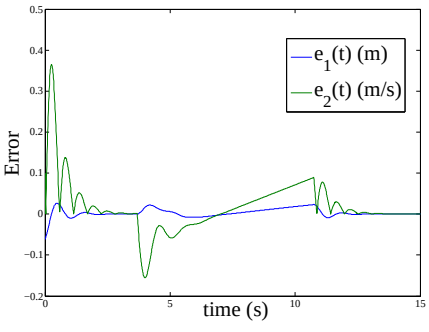

(c) Estimator 1 error

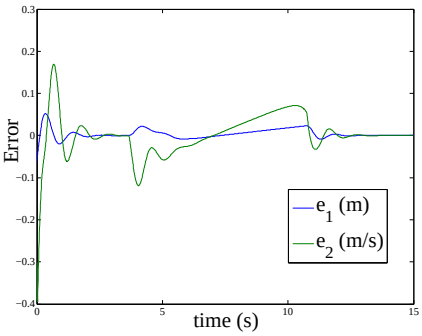

(d) Estimator 2 error

Figure 5. Estimated wind and error results for non-uniform wind-field ($K_1 = 3.5, K_2 = 35$)

D. Discussion of Numerical Results

Both estimators require a steady, uniform wind for steady-state convergence. When the wind is not uniform, the particle accelerates due to a spatial change in wind speed or direction. This change drives the error dynamics away from convergence and causes estimation inaccuracies. However, when the change in wind speed is gradual, as in the second simulation, the estimators are capable of providing a close-fitting estimate of the wind-field.

The simulated flight path presented here was smooth, in a mostly constant direction, and at a constant speed relative to the wind. When these conditions do not hold, both estimators are limited in their effectiveness. The estimators become less accurate as the speed relative to the wind s_k changes from the constant value set in the estimator. This value will likely change in time when a helicopter flies any extended path with large changes in θ_k and wind magnitude $\|f_k\|$.

The strengths of Estimator 1 include its ability to estimate both wind magnitude and direction. This allows for a relaxation of the condition that the wind remain in a uniform direction. Although a change in wind direction, like a change in magnitude, will result in a non-zero input to the error dynamics, the change will at least be taken into consideration by the estimator. Estimator 1 is incapable of providing an estimate of the change in wind-relative platform speed and is therefore not useful when trying to control s_k.

The strength of Estimator 2, is that it can calculate an estimate of the value of s_k. Also, the upper bound on the error introduced by any changes in this value is known (Section II.B). This is useful if trying to control s_k, which must stay at a steady value for accurate wind estimation. However, Estimator 2 is limited by the requirement of uni-directional wind. This means that any change in wind direction will not be taken into account by the estimator. Additionally, the wind magnitude and speed relative to the wind (Equation 7) in Estimator 2 cannot be calculated when the heading angle is at or near $\theta_k = n\pi, n \in \mathbb{Z}$ because the calculations for both $\hat{s}_k$ and $\hat{\beta}$ blow up due to the presence of $\sin\theta_k$ in the denominator of both expressions. This poses a problem when the helicopter flies in any looping path.

IV. Experimental Validation

A. Experimental Procedures

This section describes the experimental procedures used to gather tracking data of a micro-helicopter flying through a fan-produced wind-field in order to test the fit between the theoretical model and a real-world UAV platform.

The R/C micro-helicopter used in the experiment was a Blade mCX made by E-flite (Figure 6(a)). The Blade mCX is a coaxial helicopter with a rotor diameter of 190mm and a weight of 28g. Four infrared, retroreflective markers were attached to the helicopter, enabling an Opti-track infrared motion tracking system to record the position and orientation data of the vehicle throughout its flight. The motion tracking system consists of 12 infrared cameras attached to a truss surrounding a prismatic volume with dimensions of 15ft x 20 ft x 12 ft. The system has sub-millimeter tracking accuracy. By defining the four markers on the helicopter as a rigid body, the motion tracking system can record the real time position and orientation of the vehicle as it flies within the capture volume.

Yaw, pitch, and roll commands were sent to the helicopter via radio controller. The signal was sent from a hand-held, 7-channel Spektrum brand controller that is controlled through LabView. A PID controller has been programmed within Labview, allowing the operator to define a desired altitude and heading (yaw) angle.[34]

Outside of the capture volume was an array of two Lasko brand 20-inch household box fans set atop one another and adjusted to the lowest wind-speed setting. The wind-field produced from the fans was measured using a Speedtech anemometer in conjunction with the motion tracking system. An infrared marker was placed near the probe tip to allow for the recording of the precise position of each wind speed measurement. The measurement error was estimated to be ± 0.15 m/s.This was a function of the precision of the probe and the fact that the wind speed fluctuated at certain locations. For simplicity and lack of more precise measuring devices, it was assumed that the air flow was perpendicular to the fan array. This array was directed at an angle of 175.6° in the inertial frame, which was measured using the tracking system. The real component of the flow points along the negative real axis.

One hundred and ten measurements were taken at various points in the wind-field. The magnitude and inertial position of each measurement was recorded. A 3-D scalar field was interpolated from the data in

MATLAB. This interpolated wind-field (Figure 6(b)) is considered to be the ground-truth for comparison to the estimated values.

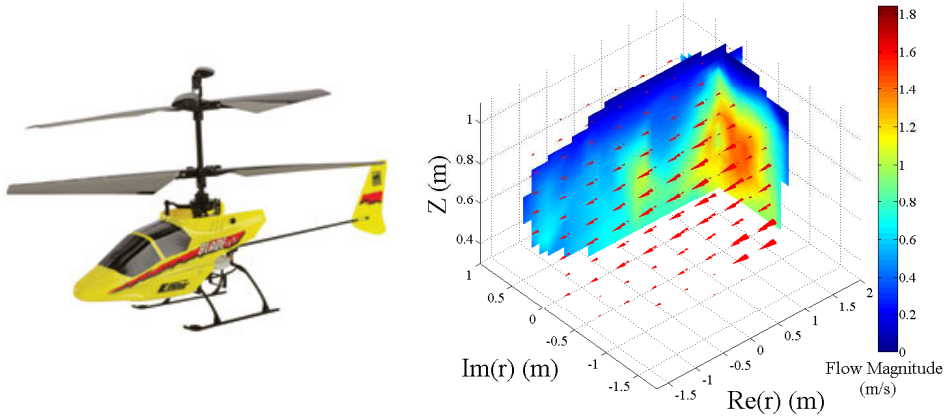

(a) E-flight Blade mCX micro-helicopter (`http://www.e-fliterc.com/`)

(b) Measured fan wind-field

Figure 6. Micro-helicopter and wind-field through which it was flown

The helicopter was flown through the wind using the LabView controller. The vehicle was set to hover at a desired altitude and yaw angle outside of the wind. The pitch was then set to a constant value to move the helicopter through the wind. It was assumed that setting a fixed pitch would give the helicopter a constant speed relative to the wind. This was found to be an inaccurate assumption and is discussed in Section IV.C. Due to the nature of the platform and the additional weight of the infrared markers, the helicopter flies best when moving backwards. Therefore, the pitch was set to a negative value so that the helicopter flew backwards through the wind. The heading θ_k was therefore defined by the direction of the tail of the helicopter.

B. Experimental Results

The tracking data from the helicopter is plotted in Figure 7(a). The estimator equations were solved using the measured values of r_k and θ_k. The values of θ_k varied in time because the yaw control did not keep the heading angle perfectly fixed. To have a relatively constant s_k, the helicopter was flown in a straight path through the flow, which resulted in data sets with a duration of only a few seconds due to the relatively small width of the flowfield.

Only the position of the helicopter in the horizontal plane was used for estimation due to the restrictions of the two-dimensional particle model. Due to the fact that an altitude controller was running in real time during the flight, the helicopter remained at a relatively constant altitude, varying only about 40 cm along the flight path. However, the actual wind speed used in the estimate comparison is the value measured at the exact three-dimensional location of the helicopter. The contribution of the altitude to the estimation error is discussed in Section IV.C. The wind angle and magnitude estimates from both estimators are shown for a single flight test in Figures 7 and 8.

For Estimator 1, the initial values of r_k and f_k were set to the exact measured position $r_{0,k}$ and a close estimate of the wind $f_k = -0.1 + 0i$ at this location. The value of s_k was set to the value of the helicopter's inertial speed before entering the flow (0.41 m/s), determined by differencing the position measurements over time. For Estimator 2, the same measured initial position $r_{0,k}$ and an initial velocity $v_{0,k} = 0$ were sent given to the estimator. The gains K_1 and K_2 were set to values of 10 and 25 respectively for both estimators.

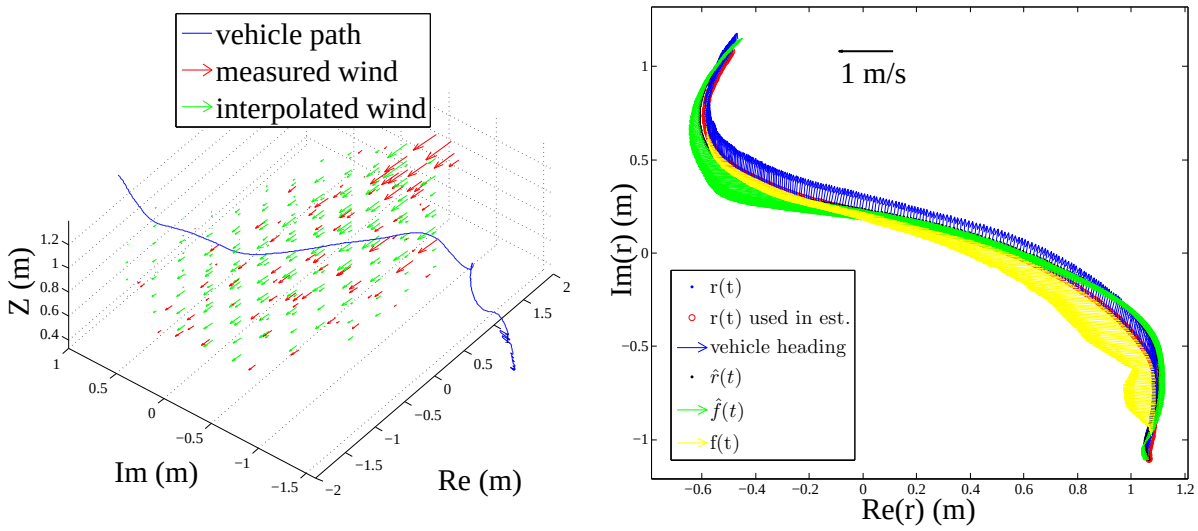

(a) Path of the helicopter flying through the wind (vector) field (b) Estimated wind plotted at the estimated position (right)

Figure 7. Visualization of helicopter flight path and wind estimates

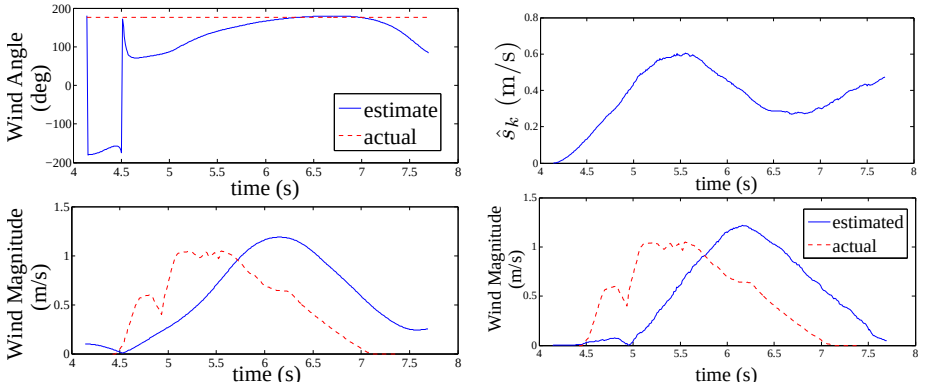

(a) Estimator 1 results (b) Estimator 2 results

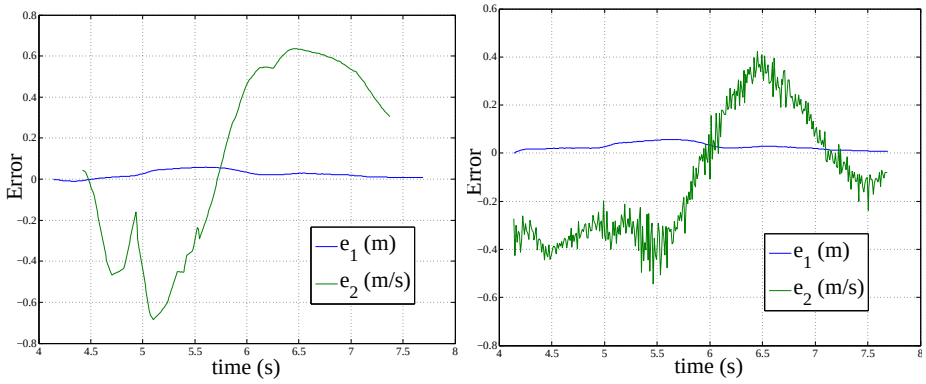

(c) Estimator 1 error (d) Estimator 2 error

Figure 8. The estimator flowfield values and errors from the experimental results.

C. Discussion of Experimental Findings

Both estimators gave wind estimates that were similar in shape to the actual wind magnitude profile, however both had significant lag. Adjusting the gains as described in Subsection C produced a faster estimate response; however, the overshoot made the magnitude estimate much too large at the peak value.

The problem posed by the lag in the magnitude estimate can be seen in Figure 7(b). The green arrows represent the estimated wind velocity $\hat{f}_k$ (from Estimator 1) and the yellow arrows represent the measured wind velocity f_k at the measured location of the helicopter. The blue arrows represent the heading of the helicopter. The black dots represent $\hat{r}_k(t)$ and the red circles represent the measured position $r_k(t)$. The spatial location of the wind estimates are shifted by about 0.5m-1m from the actual values due to the temporal lag.

Estimator 1 proved that it was capable of estimating the general behavior of both wind magnitude and angle along the flight path. However, the angle estimates were only accurate for about 1 second of data during the flight (Figure 8(a)). This angle estimate error is partially due to the short estimate window (about 2.5s) and the lack of a wider wind-field through which to fly the helicopter so that the estimator would have more time to converge to a steady-state value. The error is also caused by the discrepancy between the actual model and the idealized particle model used to develop the estimators.

Estimator 2 showed that it was also capable of generating a wind magnitude estimate that matched the general behavior of the measured wind-field. In addition, the estimator also calculated an estimate of the wind-relative speed $s_k(t)$ that varied around the initially measure value $s_k = 0.41$ (Figure 8(b)). This helps verify that the estimator is capable of providing a relatively accurate value $\hat{s}_k(t)$. This also shows that the assumption that s_k is constant does not hold. However, further tests will be necessary to determine how closely the value of $\hat{s}_k(t)$ matches the actual value $s_k(t)$. This estimated value is very useful because of its potential for use in a control law to keep the value of $s_k(t)$ as steady as possible during flight.

The magnitude lag seen from both estimators is partially due to the intrinsic properties of the estimators and the fact that they do not instantly converge in a non-uniform flowfield. The problem is exacerbated, however, because of the difference between the Newtonian particle model and the actual behavior of the micro-helicopter. In the model, the velocity of the particle relative to the flow is assumed to be purely under the control of the vehicle and is kept constant for the sake of accurate estimation. However, during experimentation it was apparent that the speed of the helicopter relative to the flow was not constant. It was assumed that sending the helicopter a constant pitch input while flying through the wind would result in an almost-constant speed relative to the wind. This was not an accurate assumption. In reality, the pitch did not remain constant while in the wind which caused unpredictable pitch and roll moments that altered the forward thrust of the helicopter along it's flight path. Additionally, the variation in the altitude of the helicopter likely contributed to a change in horizontal speed as well.

The problem of keeping the value s_k constant will require a deeper understanding of the dynamics of the micro-helicopter. We must develop a dynamic model to understand the contributions of changes in roll and pitch to the vehicle velocity and also develop a system to optimally control the altitude, yaw, and forward speed. Each of these parameters have significant coupling and understanding these relationships will therefore be necessary to improve the accuracy of the estimators. Integrating the new estimator into this control loop in order to steady $s_k(t)$ is potentially part of the solution.

V. Conclusion

From simulation, both estimators were validated for the case of steady, uniform wind and a constant platform speed relative to the wind. Further simulation showed that the estimators were still useful when the condition of flow uniformity was not met.

Both estimators were then tested experimentally using tracking data of a micro-helicopter flying through a non-uniform wind-field similar in shape to that used in the second simulation. The resulting estimates follow the behavior of the simulations and roughly match the measured wind-field; however, a temporal lag in the experimental estimates led to a significant spacial shift in the location of the estimated wind. More work will be necessary before the helicopter and estimators are capable of creating an acceptably accurate map of the wind-field.

We have successfully demonstrated the capability of the new estimator to produce an estimate of the wind-relative platform speed close to the expected value. However, more work is required to determine the

total accuracy of this estimation along the flight path. The new estimator, has shown the potential to be very valuable in the development of future control laws to steady the wind-relative speed of the platform. A more detailed model of the micro-helicopter must be created to create these control laws that will allow for increased wind-field estimation accuracy.

Acknowledgements

Many thanks to Dan Langis for helping with the data collection, Cammy Peterson for her assistance with the estimator development, and Seth Napora for the Lyapunov analysis explaining the estimator gain behavior.

References

[1]Peterson, C. and Paley, D. A., "Multi-Vehicle Coordination in an Estimated Time-Varying Flowfield," *AIAA Conf. Guidance, Control, and Dynamics (electronic)*, Toronto, Canada, August 2010.

[2]Napora, S., "Estimator Analysis," Personal communication.

[3]Langis, D. P., "Experimental Validation of Cooperative Control Laws Using a Micro-helicopter Testbed," *AIAA Region I-MA Student Conference*, April 2011.

[4]Paley, D. A. and Warshawsky, D., "Reduced-Order Dynamic Modeling and Stabilizing Control of a Micro-Helicopter," *Proc. 47th AIAA Aerospace Sciences Meeting*, January 2011, p. (9 pages).